ELSEVIER

Marine and Petroleum Geology 19 (2002) 39–53

Marine and Petroleum Geology

www.elsevier.com/locate/marpetgeo

Porosity loss in sand by grain crushing—experimental evidence and relevance to reservoir quality

Fawad A. Chuhan*, Arild Kjeldstad, Knut Bjørlykke, Kaare Høeg

Department of Geology, University of Oslo, P.O. Box 1047, Blindern N-0316 Oslo, Norway

Received 7 June 2001; received in revised form 15 November 2001; accepted 26 November 2001

Abstract

The compaction of loose sands has been tested up to high effective stresses (50 MPa). More than 50 test runs were made on five different types of sands, which were of well-sorted fine- to coarse-grained, mono-quartz and lithic compositions. The compaction curves are related directly to observations made from thin sections prepared at different stress levels. The image analyses of the thin sections show that the degree of grain fracturing increases continuously as a function of stress level. Fracturing is more intense in coarse- than in fine-grained sands and a lithic sand, fractures more readily than a mono-quartz sand in a given grain size category. Petrographic observations and grain size analyses show that, although the average grain size reduces with increasing stress level, grain fracturing is most effective in producing grains between 50 and 200 μm, which also reduces the sorting of the sands. Grain size reduction and porosity losses are higher in coarse-grained and lithic sands than in fine-grained and mono-crystalline quartz dominated sands. Fractures similar to those experimentally produced are also seen in the deeply buried Jurassic reservoir sandstones from Haltenbanken area. The experimental compaction data may provide a basis to predict reservoir quality prior to extensive quartz cementation.

Keywords: Sand; Compaction; Grain crushing; Reservoir quality

1. Introduction

Sediment compaction is important for the prediction of porosity, permeability and seismic attributes. Porosity determines, to a large extent, the density and permeability of sediments and is therefore a vital input for basin modelling. Compaction is mostly treated as a mechanical process, following classical soil and rock mechanical theory, and is then assumed a function of overburden stress (Rieke & Chilingarian, 1974), even in the deepest parts of the basin (Illiffe & Dawson, 1996; Yu & Lerche, 1996). In siliceous sediments, this may be valid for the shallow (<2 km) parts of sedimentary basins. Quartz dissolution and precipitation become more important below 2–3 km depth (70–100 °C) and therefore temperature and mineralogy are the most important control on later compaction in deeply buried clastic sediments (Bjørlykke, 1999).

Mechanical compaction of a sedimentary layer is a function of the effective stress and compressibility of the mineral framework. In a sedimentary basin, the direction of the principal stress is normally vertical but in compressive regimes, the major principal stress axis can be horizontal. In a sedimentary basin, the weight of the overlying rocks at a given depth, known as overburden total stress (σ_v), is a function of the thickness (Z) and average total density of sediments (mineral + pore fluid) (ρ), and gravity (g):

$$\sigma_v = \rho g Z$$

Some of the total overburden stress is supported by the pore (fluid) pressure (U), and the remainder is distributed over the contacts between the rock particles, and is known as the effective stress (σ'_v). The relationship between effective stress and total stress is given by (e.g. Lambe & Whitman, 1979):

$$\sigma'_v = \sigma_v - U$$

Mechanical compaction occurs via frictional slippage, rotation and sliding, and if the effective stress is sufficiently high, by crushing of sand particles (e.g. Zhang, Wong, Yanagidani, & Davis, 1990b). Grain crushing can result in tighter grain packing and reduction of primary porosity. Cathodoluminescence techniques (Dickenson & Milliken, 1995; Fisher, Casey, Clennell, & Knipe, 1999; Laubach, 1997; Sibley & Blatt, 1976) have shown that healing of fractures by quartz cement occurs in quartz rich sandstones, which suggests that grain crushing could be

* Corresponding author. Tel.: +47-228-56688; fax: +47-228-54215.
E-mail address: f.a.chuhan@geologi.uio.no (F.A. Chuhan).

0264-8172/02/$ - see front matter
PII: S0264-8172(01)00049-6

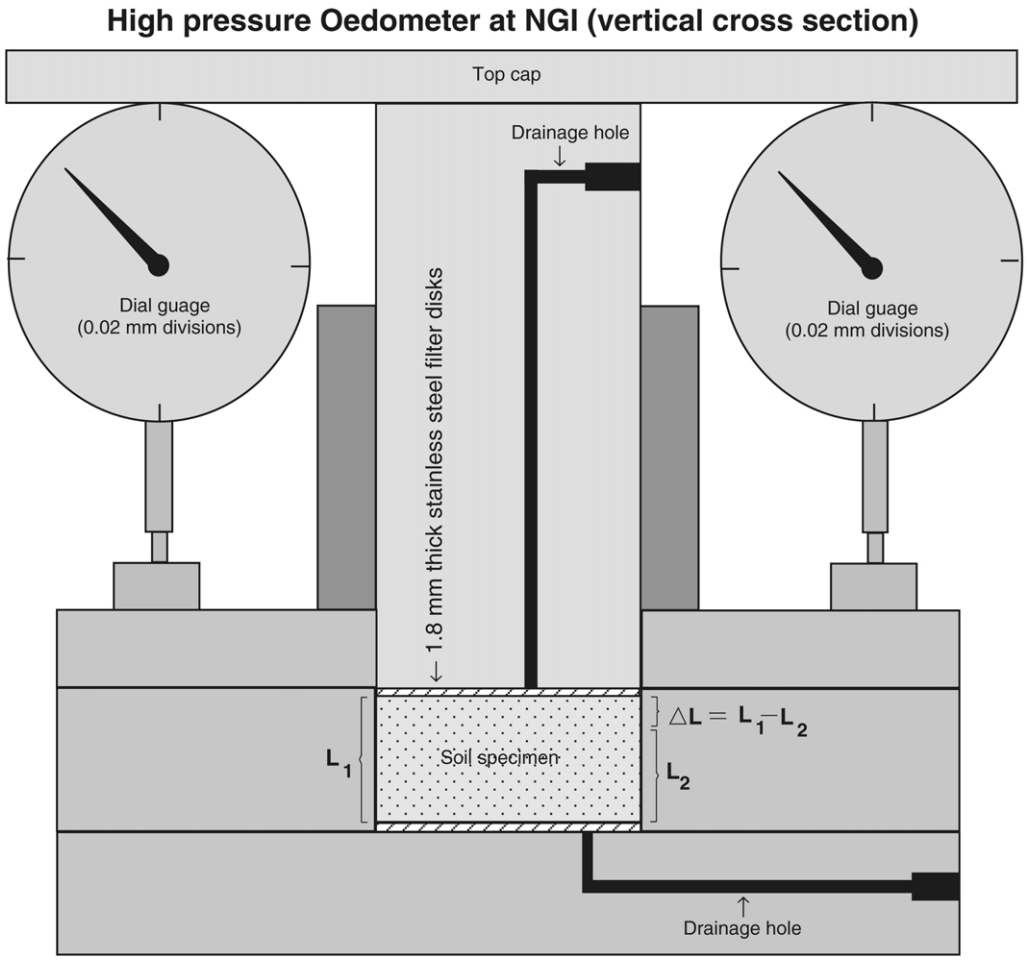

Fig. 1. Vertical cross-section of the high-pressure oedometer used in the study.

significant in naturally occurring sandstones. It is therefore important to understand the factors controlling mechanical compaction in quartz rich sandstones. Most experimental mechanical compaction has been carried out in order to solve near surface geotechnical engineering problems at relatively low levels of stress but significant work has also been conducted to understand compaction behaviour and particle crushing at elevated effective stresses (e.g. Coop, 1990; Coop & Lee, 1993; Lee & Farhoomand, 1967; Nakata, Hyodo, Hyde, Kato, & Murata, 2001; Pastana & Whittle, 1995; Roberts, 1964; Zhang, Wong, & Davies, 1990a; Zoback & Byerlee, 1976). A major shortcoming in these studies is the lack of data from petrographic observations of the compacted sands, although a few articles explain the texture of the lithic sands by using the optical microscope (e.g. Pittman & Larese, 1991). In the present study, we provide petrographic analyses of the texture of the sands compacted to effective stresses of up to 50 MPa. Sands of varying composition and grain size have been tested in order to quantify porosity losses due to mechanical compaction in sand and sandstones.

2. Experimental procedure and methodology

The one-dimensional (uni-axial) compression experimental procedure simulates sediment consolidation (compaction) under its own overburden weight in a wide basin. In this test, stress is applied along the vertical axis, while strain in the horizontal direction is prevented. Therefore, all the volumetric strain is vertical. During the one-dimensional strain condition, the horizontal effective stress is expressed by $\Delta\sigma'_h = K_0\Delta\sigma'_v$, where $\Delta\sigma'_h$, and $\Delta\sigma'_v$, are change in horizontal and vertical effective stresses, and the K_0 is the lateral stress coefficient at rest. We used a high-pressure oedometer at the Norwegian Geotechnical Institute (NGI) (Fig. 1), where only the vertical effective stresses and vertical volumetric strains were measured. Samples used in the tests were either beach sands or very loosely cemented (mainly uncemented) sands from sedimentary sequences. The samples were tested in a metal cylinder, which was 21 mm in height and 50 mm in diameter. The sand was gently packed to produce a near maximum initial porosity at the start of each test run. We attempted to ensure that the packing of the sand was constant throughout a given sample

by gradually building the specimen in thin layers. The initial porosity was calculated as:

Initial porosity

= Total volume − (Mass of sand/sand density)

The incremental loading was applied at a constant rate. The sand samples were subjected to gradually increasing levels of stress, with a maximum of 50 MPa, using a loading rate of approximately 1 MPa/90 s. Grain size analyses were performed after 10, 20, 30, 40 and 50 MPa. Thin sections were prepared from the compacted sands by allowing the sample to stay at the level of effective stress (e.g. 20, 30 and 40 MPa) for 30 min, and then unloading the sample to zero effective stress using an unloading rate of 1 MPa/45 s. The unloaded, compacted sand samples were then impregnated with dyed epoxy resin, thin sectioned longitudinally, and examined under an optical microscope. Grain size represents the graphic mean size obtained by calculating the average of the 16th, 50th, and 84th percentile diameters determined from the cumulative curves (Boggs, 1992).

3. Experimental results

3.1. Texture and composition of the sands

The five sands, which were subjected to detailed grain size and thin section analyses are well-sorted coarse-grained lithic (0.74 mm), coarse-grained mono-quartz rich (0.63 mm), medium- (0.30, 036 mm) and fine-grained mono-quartz rich (0.18 mm) sands. The mono-quartz rich sands are sub-rounded, while the lithic sand is sub-angular to angular. The mono-quartz rich sands consist of 46% mono-crystalline quartz, 4% poly-crystalline quartz and/or quartzitic lithic fragments with minor mica and feldspar, 3% feldspar, 2% slate fragments and 1% mica and clays. The lithic sand consists of 46% lithic fragments, 6% mono-crystalline quartz and 2% mica and clays and 1% chert fragments. Micaceous and clay rich lithic grains such as shale/mud clasts constitute only a minor fraction (<1%) of the lithic sand. The major rock forming lithic fragments are impure quartzite or quartzitic gneisses with non-foliated to foliated fabric having strongly sutured contacts. Most of the quartz crystallites in these lithic fragments range between 50 and 200 μm. Mica laminations present between the quartz grains constitute from 2/3 to a small fraction of the grain.

3.2. Stress vs. strain relationship in one-dimensional compression

The initial porosities in the medium- to coarse-grained sands were 45–46%, but in the fine-grained sand, it was about 49%. The porosity decreases non-linearly with increasing vertical effective stress (Fig. 2). Until about 20–25 MPa vertical effective stress, the porosity loss and compressive strain are greater in coarse-grained lithic sand than in coarse-grained mono-quartz rich sand with the same grain size. Furthermore, over the same stress interval, the coarse-grained mono-quartz rich sand loses more porosity than the fine- and medium-grained mono-quartz rich sands. The porosity values at 25 MPa are ~31% for the coarse-grained lithic, ~33% for the coarse-grained mono-quartz and ~36–37% for the medium-grained mono-quartz sands. The fine-grained sand has a higher initial porosity and a higher porosity value at 25 MPa (~38%). However, both the strain increase and porosity loss become rather similar after 20–25 MPa, regardless of the grain size and composition.

In order to quantify the stiffness of the sand at different stress levels, the constrained modulus value has been calculated, which is $M = \Delta\sigma'_v/\Delta\varepsilon_v$, where M is the tangent constrained modulus at a given stress level, $\Delta\sigma'_v$ the incremental vertical effective stress beyond σ'_v, and $\Delta\varepsilon_v$ is the resulting additional strain as a function of original height of the sample (shortening of the sample).

For σ'_v less than 5 MPa, the constrained modulus increases sharply and reaches a maximum at 4–6 MPa. Lithic sand shows lower values and is more compressible than mono-quartz rich sands. In the same stress range, the increase in modulus is more rapid in the coarse- than in the fine-grained mono-quartz sand. The compressibility of the sands changes significantly due to grain crushing when σ'_v reaches 4–6 MPa. The modulus decreases dramatically for the coarse-grained mono-quartz sand at stresses between 4 and 10 MPa, after a peak value at 4 MPa. The peak values of the modulus are higher in the coarse- than in the medium-grained sand and the modulus starts to increase gradually once again in the coarse-grained mono-quartz sands at about 15 MPa. The stress level where the increase in the modulus begins is lower in coarse-grained sand than in medium-grained sands. The increase is more rapid in the coarse sands than in the medium-grained sands. However, the modulus continues to increase in the fine-grained mono-quartz and coarse-grained lithic sands, without showing a peak value of modulus. The modulus value is higher in the coarse-grained sands than the medium-grained sands at the end of loading at 50 MPa.

3.3. Frequency of grain breakage

The amount of grain breakage is calculated from the difference in the particle size distribution curves as measured before and after loading, by using standard sieve analyses. We analysed one coarse-grained lithic and three coarse- to medium-grained quartzitic sands for grain breakage at different stress levels. The grain size analyses clearly show that the grain size decreases with increasing vertical effective stress in all the sands (Fig. 3).

A parameter that has been used to measure the particle breakage, is the ratio D_{15i}/D_{15a}, where D_{15i} and D_{15a} are the diameters for which 15% of the original and loaded samples,

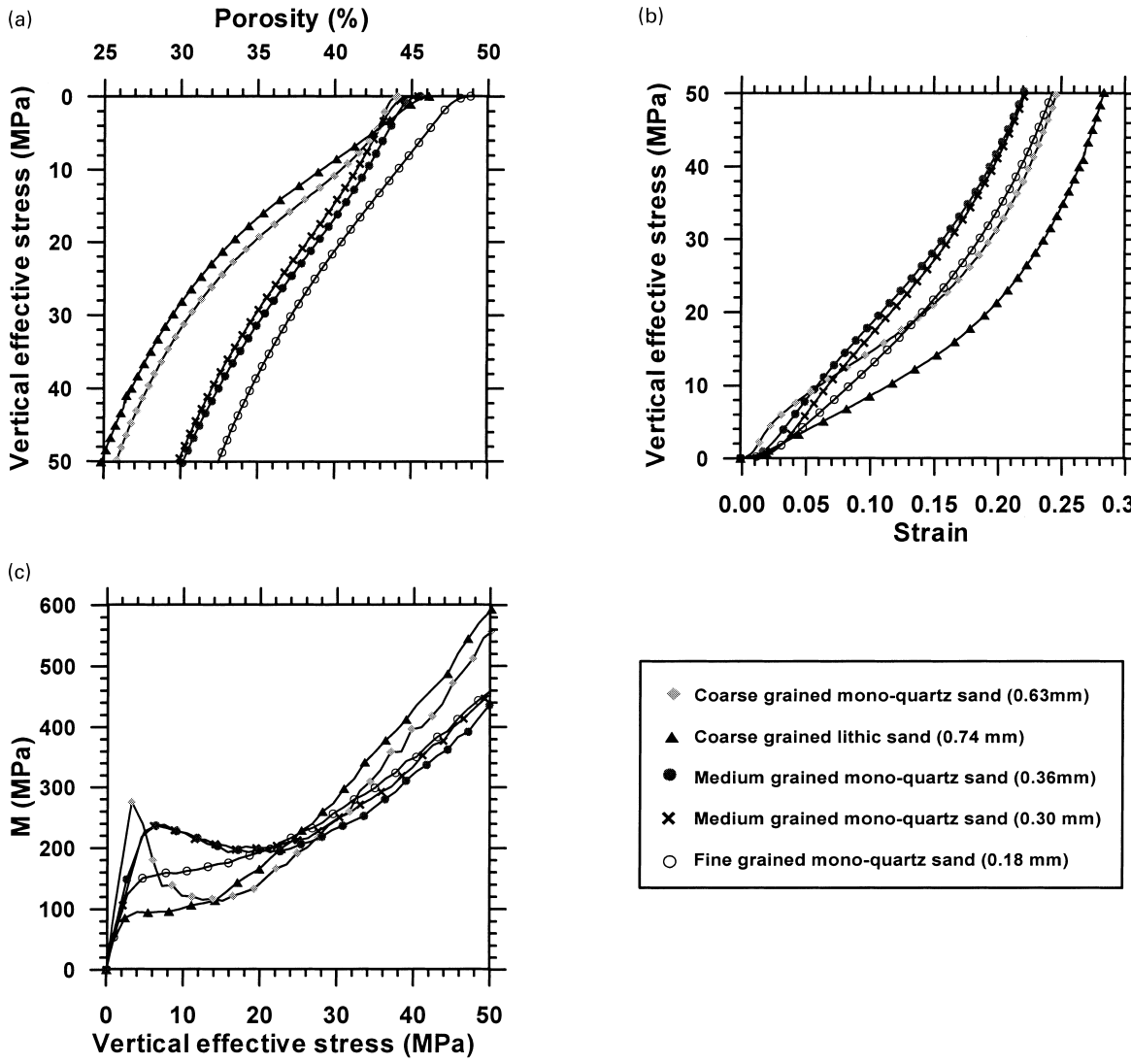

Fig. 2. Vertical effective stress vs.: (a) porosity; (b) strain; (c) constrained modulus.

respectively, are finer (Lee & Fahroomand, 1967). The test results from three mono-quartz sands show that the increase in the ratio D_{15i}/D_{15a}, with increasing stress, is more pronounced in coarse- than in medium-grained sand. In addition, with increasing stress, the same ratio, measured from two coarse sands with different mineralogy, shows a greater increase in lithic sand than in mono-quartz sand. The overall decrease in grain size with increasing stress level also affects the sorting (D_{60}/D_{10}), which tends to become poorer in the coarse and lithic sands than in the mono-quartz and fine sands (Fig. 4).

3.4. Petrographic description of compacted sands

Thin sections were prepared after each of the sands that had been subjected to 10, 20, 30 and 40 MPa vertical effective stress. The thin sections were analysed by an image analysis programme as well as by standard petrographic modal analyses. A binocular microscope with a ×4 objective and a ×10 eyepiece was used, and the microscope was mounted with computer-linked video camera. Images from the thin sections were analysed using a ZEISS software program. The fractures inside the grains include 'closed' and 'open' fractures. Open fractures are detectable by blue dye resin, and porosity can be seen under the optical microscope. Such visible secondary porosity corresponds to widths of 10–50 μm. Closed fractures are considered to be those where no detectable porosity is observed. The fractures normally radiate from grain contacts; however, fracture openings towards the open pore are also common. On the basis of morphology grain fractures can be divided into two types:

1. simple fractures;
2. complex fractures.

In simple fracture types, only one fracture is present within the grain (Fig. 5(A) and (B)). In the complex types,

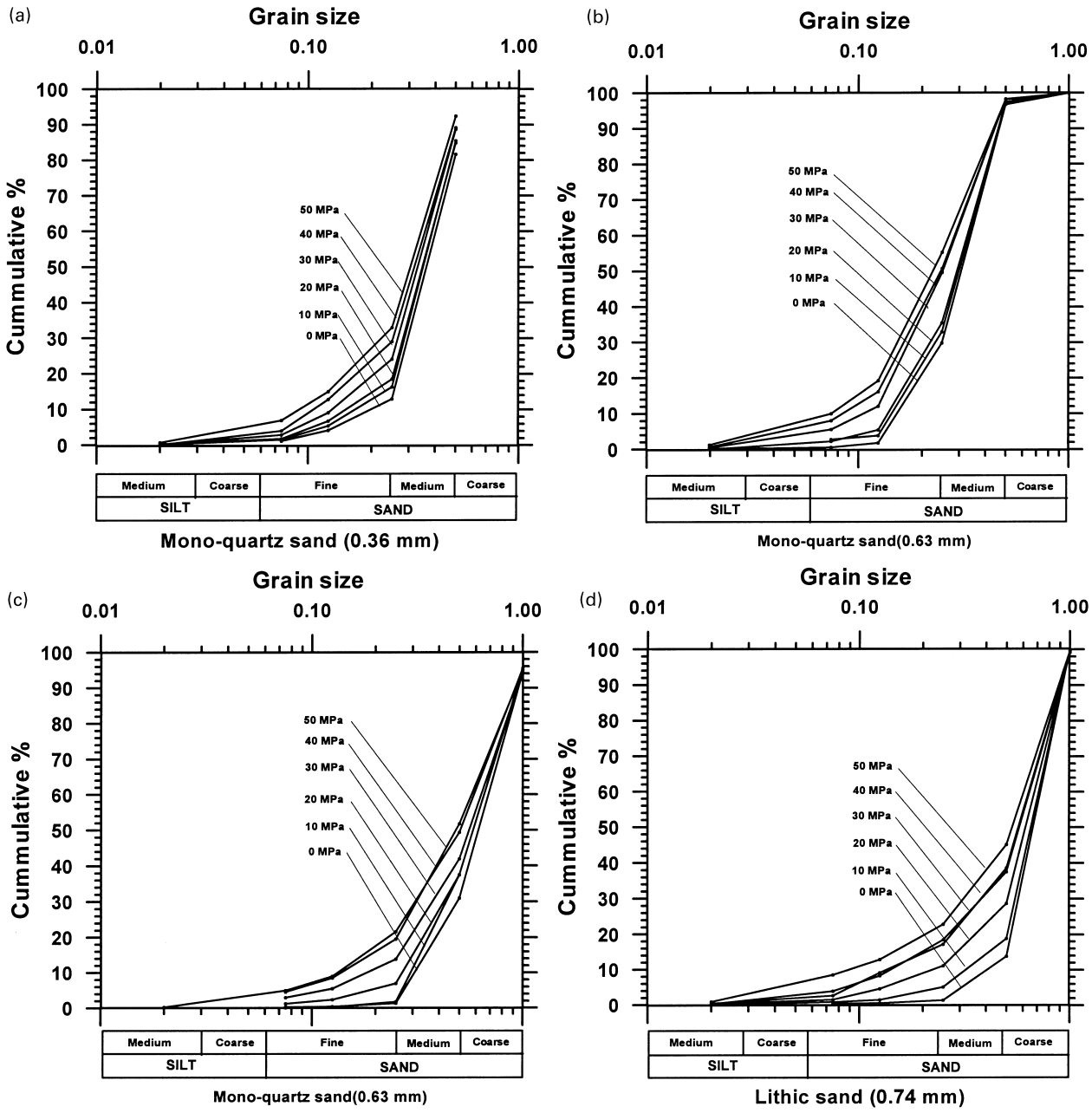

Fig. 3. Grain size distribution as with increasing vertical effective stress in: (a, b) medium-grained mono-quartz sand; (c) coarse-grained mono-quartz sand; (d) coarse grained lithic sand.

a fracture network is developed which either forms a 'cone crack' pattern near the grain contacts (Fig. 5(a), (d)–(f)) or an irregular fracture pattern that can be at the grain contact or within the grain (Fig. 5(c) and (f)). The cone crack pattern near the grain contacts are reminiscent of tensile indentation fractures usually referred to as 'Hertzian fractures' (Zhang et al., 1990a). During analyses, the fractures were marked with the help of a 'draw line' option by tracing one side of the open fracture. The degree of fracturing in a sample was determined by measuring the number of fracture covering pixels per unit area examined. The analyses include ten images per thin section, representing almost the entire thin section.

3.4.1. Mono-quartz and lithic sands

The thin section analyses show that prior to loading, the sands have very few fractured grains. The number of fractured grains and degree of fracturing, as measured by modal and image analyses, respectively, increase with stress level in all the sands (Fig. 6(a)–(c)). The degree of fracturing is more pronounced in the coarse- than in the fine-grained mono-quartz sands. Lithic sand shows more frequent

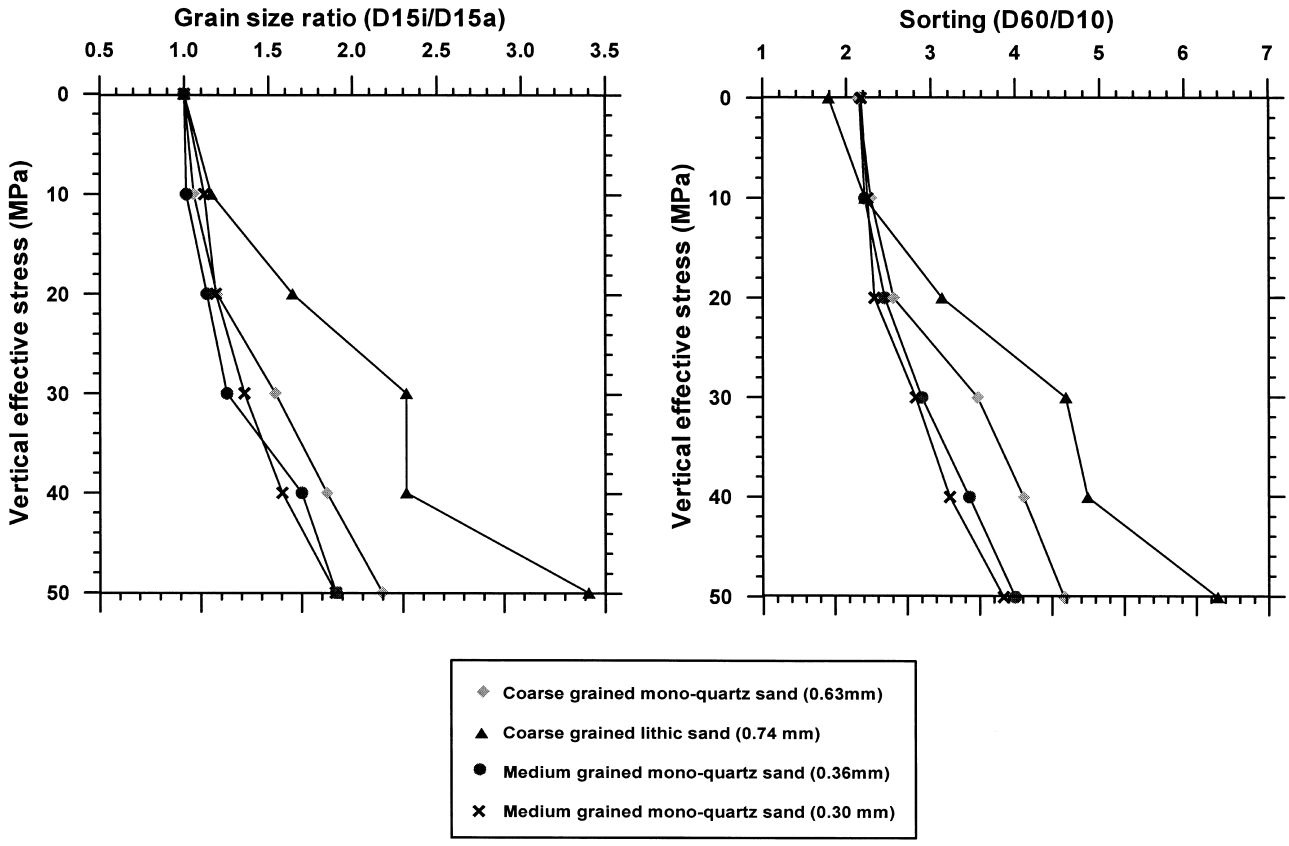

Fig. 4. The grain size ratio D_{15i}/D_{15a} and sorting D_{60}/D_{10} plotted against vertical effective stress in the studied sands.

fracturing than mono-quartz sand and the fracture pattern is of a complex type. In lithic sand, the poly-quartz and lithic grains are intensely fractured and disintegrate into smaller grains at stresses higher than 30 MPa. The intensity of simple fractures increases with stress level in all the sands but complex and open fractures occur mainly in the medium- and coarse-grained sand at 30 and 40 MPa stress levels. Such fractures are almost absent at 10 MPa, with only minor development at 20 MPa (Fig. 5(a)). The fracturing of sand grains is very unevenly distributed within a single thin section and the relationship of the fractured grains to one another is highly variable. Most of the grains in a thin section are in contact with each other and remain non-fractured but grains that are fractured at all available contacts with neighbouring grains (Fig. 5(a), (b) and (f)) are also common. A third type of fracture distribution is also prominent after 20 MPa, in which a grain with simple and complex fracturing abuts a non-fractured neighbouring grain (Fig. 5(a) and (d)). The detailed observations suggest that, in most cases, the grains are pulled apart producing only a small opening without major offsets. A few mono-quartz grains are fragmented and squeezed into the pores (Fig. 5(f)).

The lithic sand shows a complex fracture pattern within the grains at all stress levels. The micaceous and clay rich grains such as shale/mud clasts, which constitute only a minor fraction (<1%) of the lithic sand, show highly ductile behaviour and the grains deform plastically by bending or compacting into pores. The petrographic studies of thin sections prepared at different stress levels show that the deformation of grains results from the separation of individual quartz crystals. A few fractures are developed along the sutured grains during the initial stages (Fig. 7(c) and (d)), and with increasing stress level up to 40 MPa most of the poly-crystalline quartz grains show disintegration of the primary grains (Fig. 7(d)–(f)). Breakdown of lithic grains occurs preferentially where quartz grains are in contact with mica flakes, while the quartz–quartz sutured contacts are more or less intact in the same grain (Fig. 7(f)). The brittle grain fracturing associated with mica–quartz and quartz–quartz contacts is widespread in the lithic sand. This is confirmed by image analyses of the compacted sands, which also indicate a higher degree of fracturing in the coarse-grained lithic sand than in the coarse-grained mono-quartz rich sand.

3.4.2. Artificially mixed sands

Samples of sands for testing were also prepared by mixing different grain size fractions and also by adding mica/clays. In one mix, medium grained (0.30 mm) sand was mixed with coarse-grained (0.63 mm) mono-quartz sand in equal proportions (wt%). Image analyses, combined with petrographic observations and modal analyses, show that the degree of fracturing is higher in medium size grains than in coarse grains in the same sample. This is especially

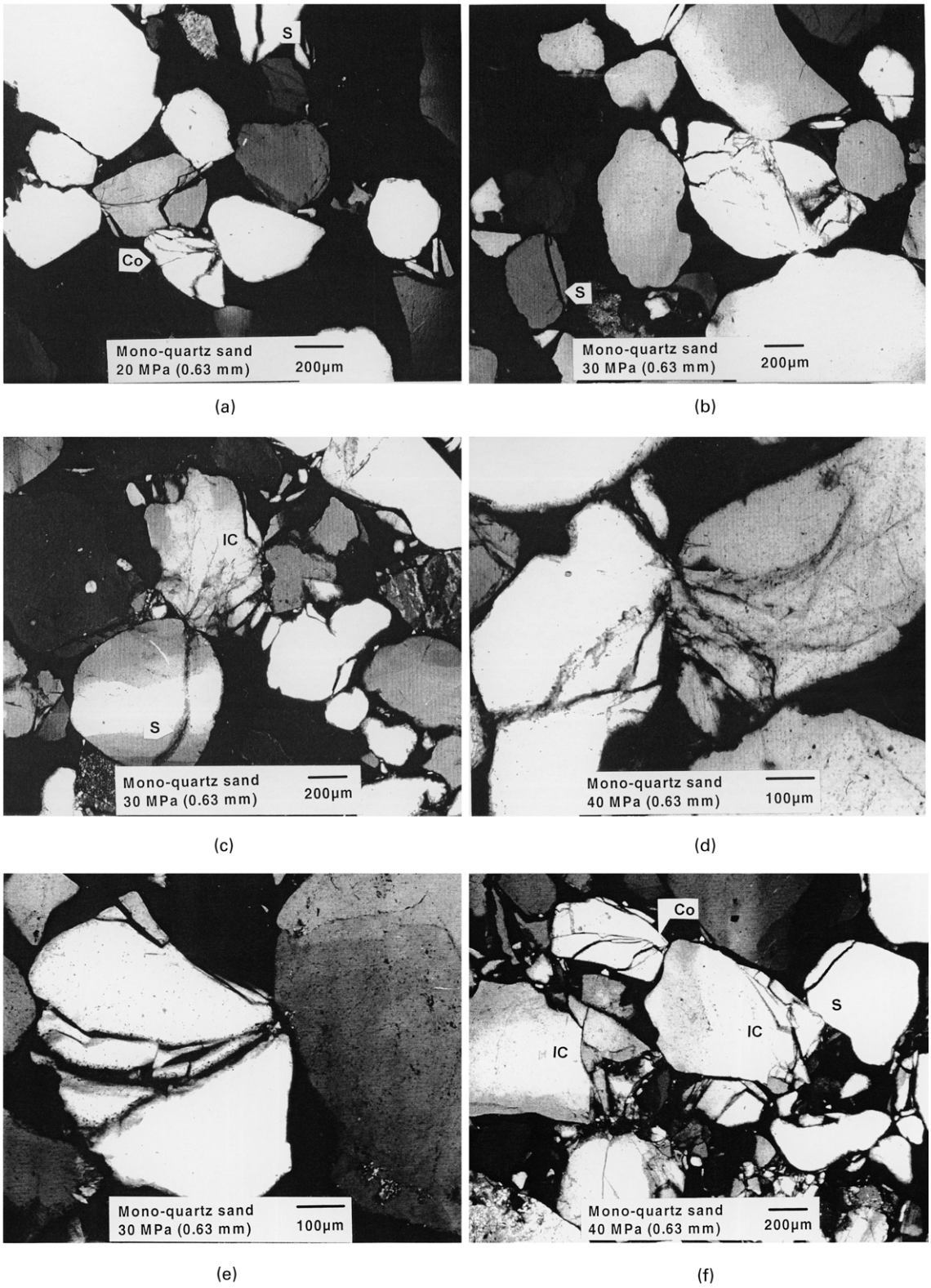

Fig. 5. Photomicrographs showing grain fracturing in experimentally compacted coarse-grained (0.63 mm) mono-quartz sand. (a, b) Complex type of grain fracturing at all contact points, with simple fracture (S) and cone fracture (Co); (c) simple fracture (S) and irregular complex fracture (IC); (d, e) close ups of cone type fractures; (f) heavy fracturing showing simple (S), cone (Co) and irregular complex (IC) fracture types. All photomicrographs were taken with X-nicols.

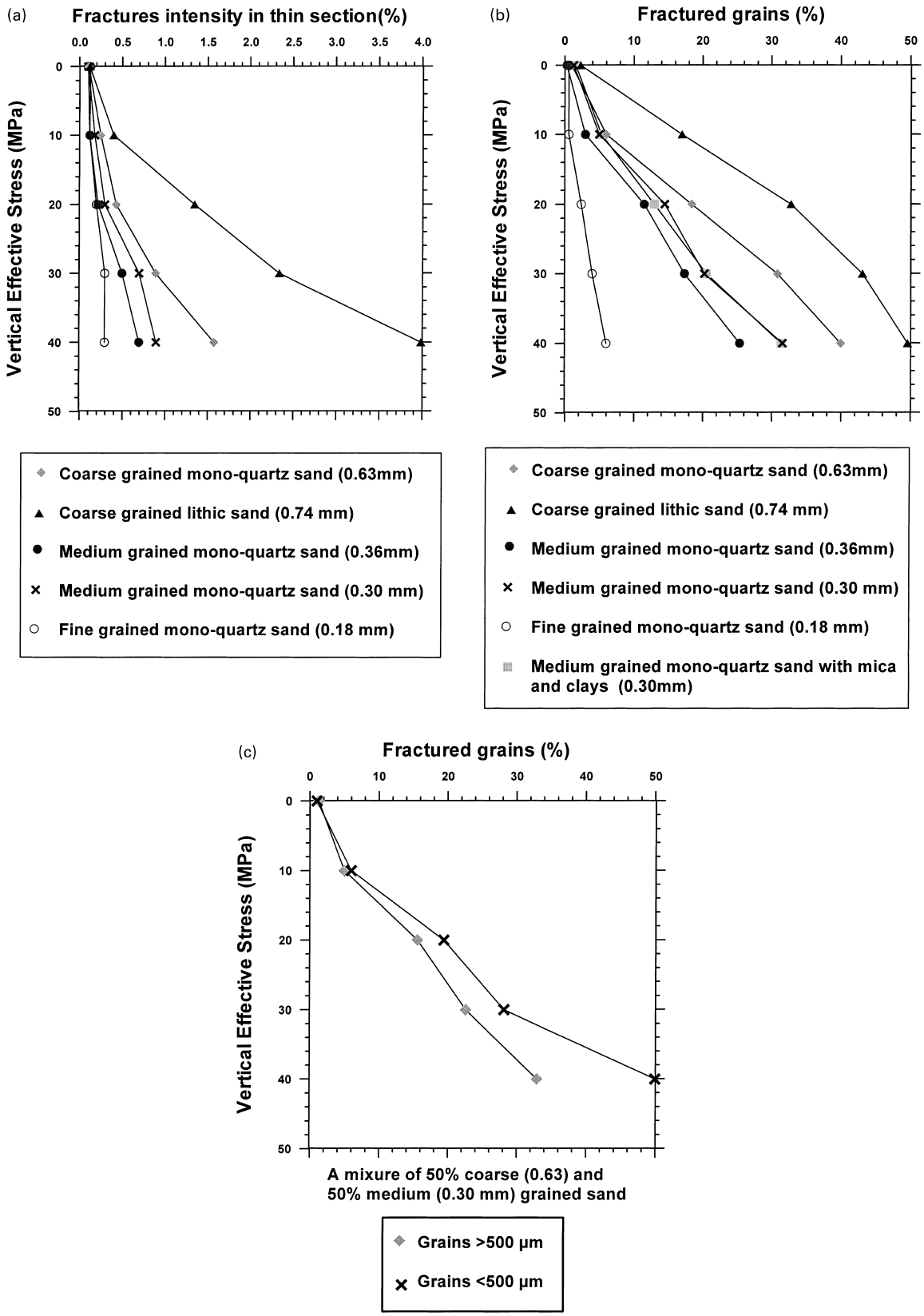

Fig. 6. Degree of grain fracturing in various sands as measured from thin section petrography using: (a) image analysis programme; (b, c) modal analyses of thin sections.

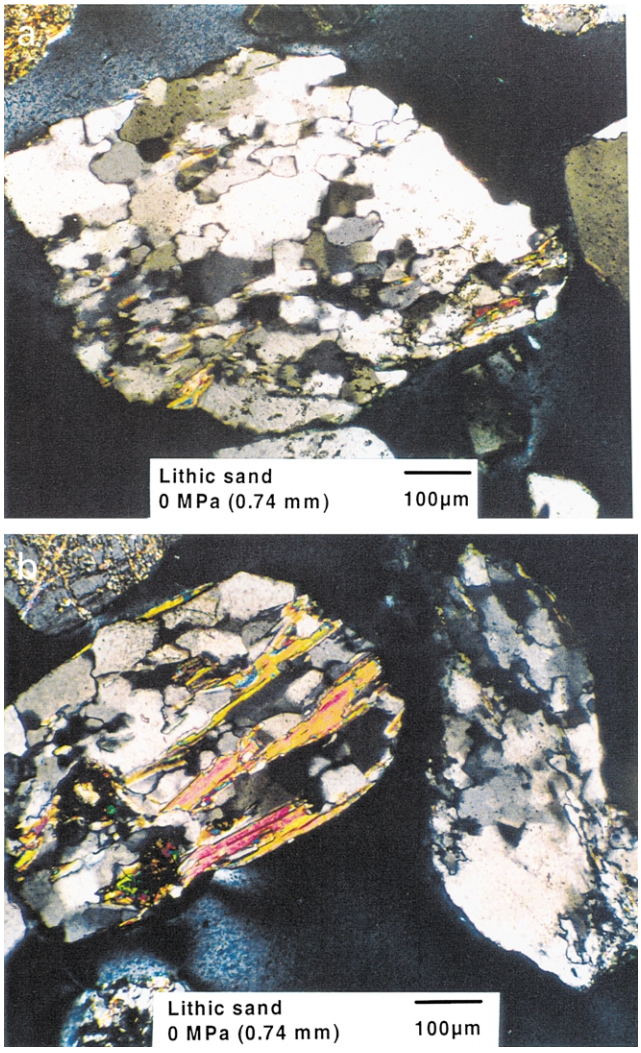

Fig. 7. Photomicrographs showing grain fracturing in experimentally compacted coarse-grained (0.74 mm) lithic sand at different levels of stress. Initial sand with strongly sutured, partially foliated lithic fragment with: (a) minor mica; (b) 25% mica in the left grain, while mica absent in the right grain. Increasing degree of disintegration of lithic grain as in (a) at 10 (c), 20 (d) and 40 (e) MPa stress levels. Development of fractures in lithic grain with mica at 40 (f) stress level, similar to original sand grain in (b). All photomicrographs were taken with X-nicols while PPL photomicrographs shown on the right hand side in (c)–(f).

true at stresses higher than 20 MPa. In addition, the coarse grains show more grain contacts with the neighbouring grains than the medium grains, and the number of grain contacts in any given grain size category increases with increasing effective stress level (Table 2).

To evaluate the effect of mica and clays, a new sand was prepared by adding 5% clays and 5% mica into the medium-grained (0.3 mm) mono-quartz rich sand. The results show that the degree of grain fracturing and number of fractured grains is rather similar to that for the original medium grained (0.3 mm) mono-quartz rich sand. The porosity loss is enhanced in the initial stage in the clay and micaceous sand, but the overall grain fracture distribution is not effected by the small amount of clay and mica. Therefore, the degree of grain fracturing from the clean sands tested in this study can be comparable with the naturally existing sands from the sedimentary basins.

3.5. Petrographic and cathodoluminescence imaging of reservoir sandstones

We analysed 10 thin sections from deeply buried (>4.5 km) Jurassic reservoir sandstones from well 6506/12-10 at Haltenbanken area, Mid-Norway. The sample depths vary from 4959.0–5096.8 m. Standard petrographic analyses show that the samples are mainly sub-arkosic arenites with less than 5% matrix. Median grain diameter varies between 0.2 and 1.1 mm with trask coefficient of 1.2–1.5. The main rock forming detrital minerals are quartz, feldspar, minor rock fragments and muscovite. The major authigenic minerals are quartz, illite and grain coating chlorite. Samples without grain coating chlorites are heavily cemented with quartz. However, samples with extensive grain coating chlorites show wide variation in quartz cement content. The fine- to medium-grained samples contain well-developed coatings with little quartz cement. The coarse-grained samples contain well-developed coatings with intervals of extensive quartz cement. In coarse-grained samples, some areas contain quartz cement, which is not in optical continuity with the detrital grains. Analyses were conducted at the Department of Geology, University of Oslo with a Joel 840-Scanning Electron Microscope (SEM) at 15 nA sample current and 15 kV accelerating voltage in order to identify fractures healed with quartz cement. Back scattered (BSE) and cathodoluminescence imaging (CL) were used. Standard polished thin sections were coated with carbon for CL imaging. The CL microphotographs show that detrital quartz has bright and weak luminescence (Fig. 8). However, some grains do not show luminescence. The authigenic quartz shows grey colour, which is darker than the detrital grains. Authigenic quartz is present mainly in the form of overgrowth, but it is also present as of cement filling the fractures and growing into the pores (Fig. 8(c)). It can be seen that the fracture does not cut the cement; therefore, the fracturing of these grains clearly predates quartz cementation. The analyses show that in samples without chlorite coatings, grain fracturing is common in medium- to coarse-grained sandstones, but is rarely observed in the fine-grained sandstones. In the coarse-grained samples with chlorite coatings, detrital quartz grains contain numerous fractures filled with quartz cement (arrows) (Fig. 8(b) and (c)).

4. Discussion of results

4.1. Grain crushing and compaction in sands

4.1.1. Onset of grain crushing

The results of the experimental compaction show that the sands stiffen with increasing vertical effective stress up to

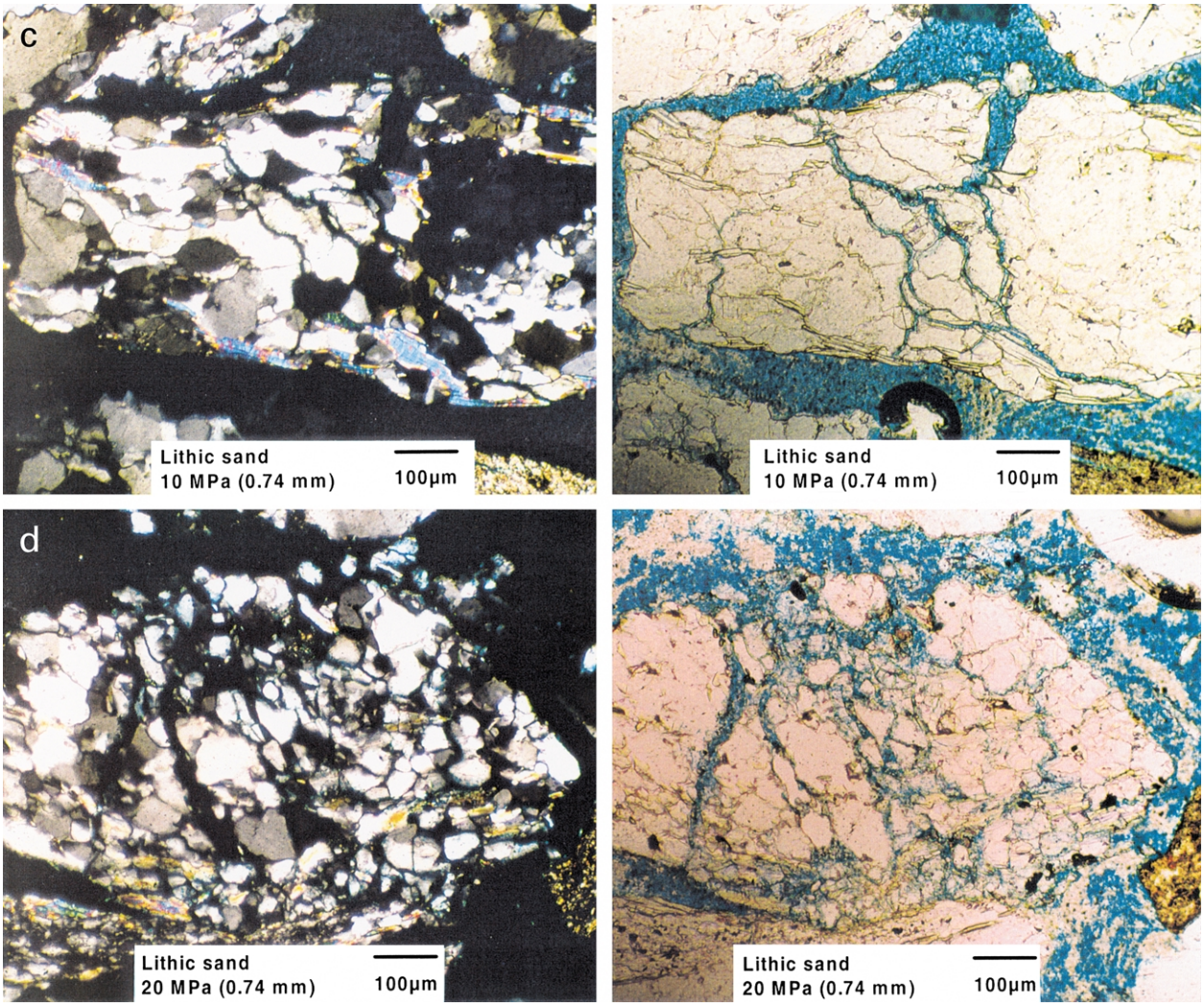

Fig. 7. (*continued*)

2–6 MPa, and this stiffening is shown by the gradually increasing constrained modulus (Fig. 2). The initial strain (compaction) results mostly from rotation and movement of grains past one another. The medium- and coarse-grained mono-quartz sands show an increase in strain (a plateau) at a low stress level, where the sand loses its stiffness (Fig. 2) (Lambe & Whitman, 1979). The peak value of constrained modulus is reached at 2 MPa in the coarse-grained sand and 6 MPa for medium-grained sands (Fig. 2). The peak value indicates that the grain framework even at low stresses (<6 MPa) loses its rigidity due to minor fracturing of grains, which might be difficult to quantify from thin section analyses, but is sufficient to abruptly increase the strain. Fracturing in a small percentage of the grains changes the stress distribution among the neighbouring grains, making the sand framework unstable and resulting in significant grain slippage and rotation, as the grain packing remains very loose at these low stresses. However, a peak value of constrained modulus is absent when the grain size is fine and the sand is lithic (Fig. 2), and this is due to higher strains in these sands. Higher strain in the coarse-grained lithic sand than in mono-quartz rich sand, results from the relatively higher degree of grain crushing in the lithic sand. However, higher strain in the fine-grained sand than in coarse-grained sand is due to rotation and reorientation of the angular grain framework of the finer sands.

4.1.2. Grain crushing after 10 MPa

The intensity of grain crushing in the medium- and coarse-grained sands increases with increasing stresses after 10 and 20 MPa in lithic and mono-quartz rich sands, respectively. This is in agreement with the results from experimental compaction of sand (e.g. Coop & Lee, 1993; Hagerty, Hite, Ullrich, & Hagerty, 1993; Lee & Farhoomand, 1967; Nakata et al., 2001; Roberts, 1964). These authors suggest that a yield point occurs between 10 and 20 MPa, which is related to the initiation of marked particle crushing. Grain size analyses performed at different stress levels in different sands support the thin section analyses and show that there is a very gradual decrease in the average

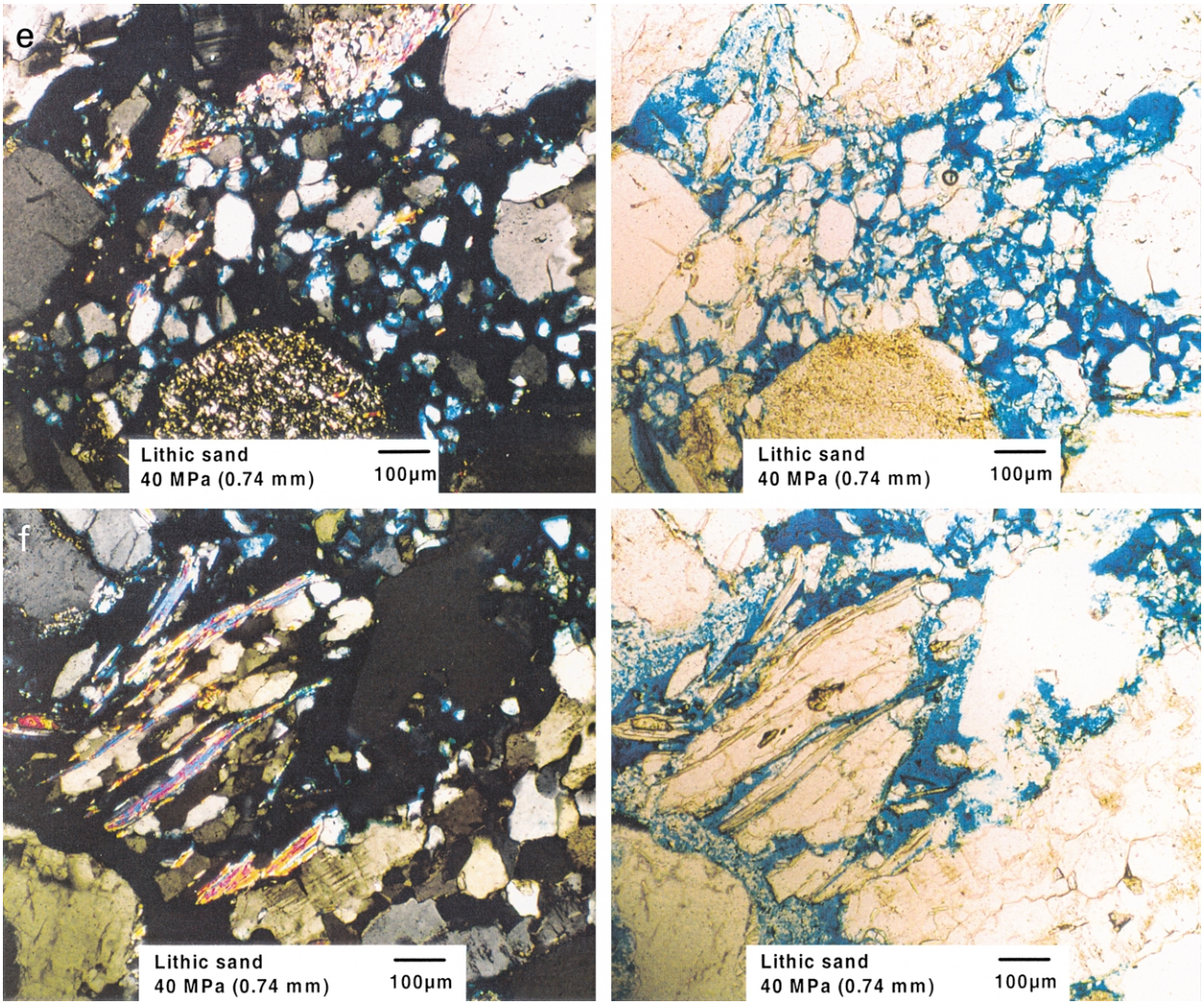

Fig. 7. (*continued*)

grain size with increasing vertical effective stress, suggesting that grain fracturing is operative (Figs. 3 and 4). At higher stresses (>20 MPa), the fractures do not show any larger offsets (Fig. 5). This indicates that the sand framework is very stiff so that the relative movement between the grains is minor despite the higher degree of grain fracturing. Therefore, at higher stresses (>20 MPa), compression occurs gradually.

4.1.3. Grain fracturing related to grain size and compositional variations

The total porosity losses within the coarse-grained sands, when loading from 0 to 50 MPa, are higher in the lithic sand than in the mono-quartz rich sand. Under similar stress conditions, the fine- and medium-grained sands lose the least amount of porosity (Table 2). The initiation of brittle fracturing at relatively low stresses (10 MPa) and its greater intensity in lithic sand than in mono-quartz rich sands, results in the higher porosity losses associated with lithic sands. Experimental compaction by Pittman and Larese (1991) also showed that the presence of lithic fragments in the sand enhances compaction. Similarly, the higher degree of grain fracturing in the coarse-grained sand compared to the finer sands results in higher porosity losses in the coarser sands. The grain size analyses are consistent with petrographic observations and show that the decrease in grain size due to grain crushing is more intense in lithic sand than in mono-quartz sand and in coarse- than in fine-grained sand (Fig. 4). Higher porosity loss in lithic sand is due to the weakness of the grains, which disintegrate into finer grains (mainly 50–200 μm). The number of grains and inter-granular contacts per unit of cross-sectional area is smaller in specimens with larger particles, and there is consequently a higher force per grain contact. It has been suggested that the average inter-particle stress level would vary inversely with the number of inter-particle contacts and would be higher for specimens with larger particles (Hagerty et al., 1993). However, Hertzian contact theory for spherical grains has been used by several authors to suggest that contact stresses are independent of grain size

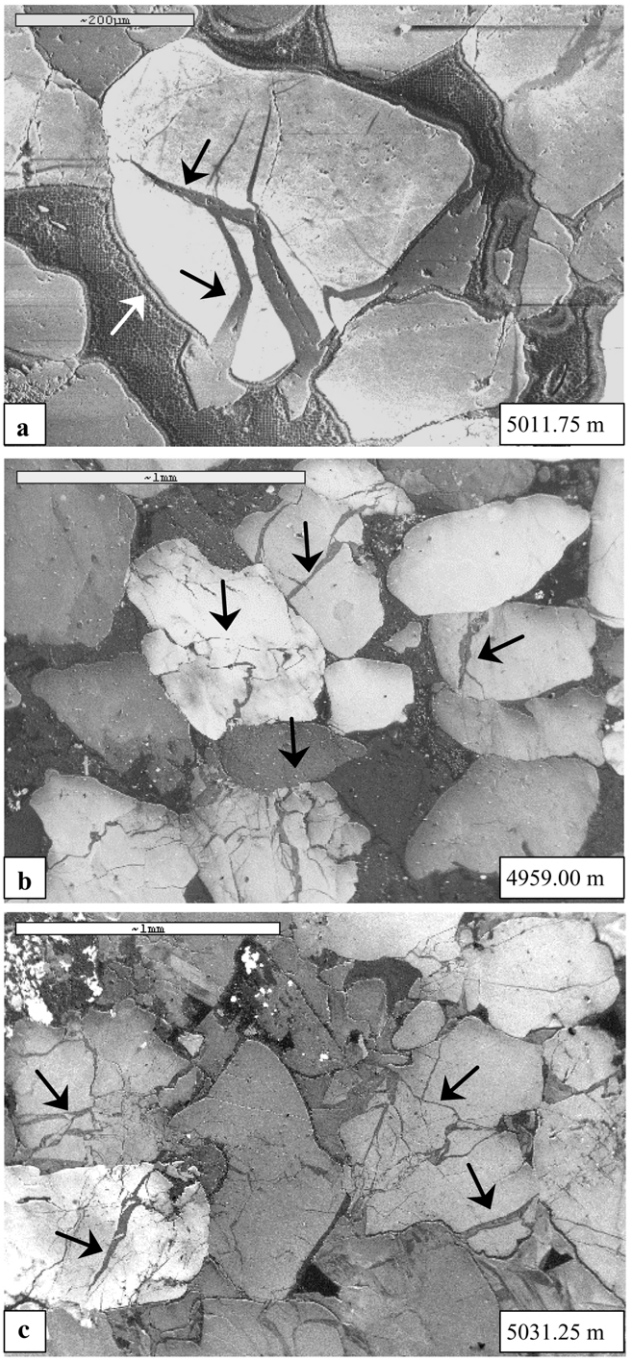

Fig. 8. Photomicrographs of Tilje Formation from well 6506/12-10 at Haltenbanken area showing: (a) CL image of authigenic quartz filling the fracture in detrital quartz grain, marked by black arrow. White arrow points towards chlorite coating; (b) and (c) CL image of coarse-grained sandstones showing numerous fractures healed with quartz cement.

(e.g. Brzesowsky, 1995; Johnsen, 1985). This is because the larger grains will have larger grain contact area resulting from higher stresses. The increase in grain fracturing with grain size is, in the Hertzian theory, often explained by the fact that the pre-existing crystal imperfection increases with the grain size. This enhances the probability of grain fracturing with increasing grain size. Traditional Hertzian contact models are based on the assumption that the grains are spherical (e.g. Johnsen, 1985; Zhang et al., 1990a). This is hardly the case in naturally occurring sands. Thin section analyses show that the grain contact areas vary considerably in size inside a given specimen depending upon the grain shape. Therefore, the contact stress varies significantly in magnitude. In coarse-grained sands, sharp non-spherical point grain contacts are common. This could also contribute to higher frequency of fracturing in the coarser grain sands, in addition to the higher frequency of pre-existing crystal imperfections.

Porosity loss is rather similar in the fine- and medium-grained sands but the degree of grain crushing is significantly higher in the medium-grained sand than in the fine-grained sand. Porosity loss in the fine-grained sand is mainly due to grain reorientation and sliding, while grain crushing causes higher porosity losses in the medium-grained sand. Therefore, comparable porosity loss, with different causes, occurs in the fine- and medium-grained sands.

The differences in porosity values due to higher degree of grain crushing in coarser and lithic sands are most apparent up to 25 MPa, but porosity–stress curves become almost parallel after 25 MPa (Fig. 2; Table 2). Therefore, initial sand texture and composition play a vital role up to 20–25 MPa stress level. Higher degree of grain crushing in the coarser and weaker sands promotes compaction. The finer material thus generated is difficult to crush, which suppresses compaction. Grain crushing can thus be considered a part of a self-organising process, where the sand is adopting itself to higher stresses.

4.1.4. Inter-granular fracture distribution

The complexity of fracture patterns and the inhomogeneity of fracture distribution inside the sand is due to the interaction of local stress fields induced at the contact planes and also the variations in grain strength. Some grains are therefore more easily broken than others are in the same sample (Fig. 5(e)). When mixing medium- and coarse-grained sands, the medium grains show more fracturing than the coarse grains (Fig. 6(d)), although the possibility of inherited micro-fractures is greater in the coarser grains and could promote more intense grain fracturing (Zhang et al., 1990a). However, the more frequent breakage of medium grains than the coarse grains might indicate that, where finer grains are present, the coarser grains are more confined by other grains. Thin section analyses show that the coarser grains are in contact with more neighbouring grains, thus distributing the stress at more contact points (Table 1). The presence of several grains around the coarser grains causes the local stress field to act more like an isotropic compression of the coarser grain. The smaller shear stresses on the coarser grains, therefore delay fracturing relative to those with medium grains size.

Table 1
Porosity values, and porosity losses at different stress levels and intervals

Composition	Grain size D60 (mm)	Mean grain size (mm)	Sorting	Initial porosity (%)	Por. at 25 MPa (%)	Por. at 50 MPa (%)	Por. loss 0–25 MPa (%)	Por. loss 25–50 MPa (%)	Por. loss 0–50 MPa (%)
Mono-quartz	0.19	0.18	0.04	48.8	38.9	32.5	10.6	6.4	16.4
Mono-quartz	0.37	0.36	0.12	44.5	34.6	28.3	9.9	6.4	16.2
Mono-quartz	0.33	0.30	0.10	45.4	36.3	29.9	9.4	6.4	15.5
Mono-quartz	0.68	0.63	0.14	44.7	32.8	26.7	15.4	6.1	18.0
Lithic	0.73	0.74	0.20	46.1	31.2	24.8	17.7	6.3	21.3

4.2. Implication for reservoir quality

The results of the experimental compaction of different types of sand described earlier can be used in the prediction of porosity loss in sedimentary basins. The grain size and composition of sand a play vital role in determining the porosity value at any given vertical effective stress level (Table 2). In many sedimentary basins, like the Norwegian Continental Shelf, quartz cementation normally starts at about 90–100 °C and becomes increasingly important after 2 km burial depth (Lander & Walderhaug, 1999). Quartz cement is one of the major porosity deteriorating factors in the deeply buried sandstones. The effective stress at 2 km is ~25 MPa. Here we assume average grain density = 2.2 g/cm^3; density of water = 1.02 g/cm^3, and hydrostatic pore pressure condition. The experimental compaction results show that cleaner fine-grained sands can have ~6% points higher porosity than coarse-grained sands at 25 MPa, i.e. at the onset of quartz cementation. These differences must be considered during modelling of quartz cementation. The degree of grain crushing in an uncemented sand becomes increasingly important after 10–20 MPa, but mechanical compaction will stop when quartz or carbonate cementation have increased the rock strength sufficiently. Cathodoluminescence microphotographs show fractures healed with quartz cement (Fig. 8(a)). These kinds of fractures are common in the medium- to coarse-grained sandstones, but are rare in fine-grained sandstones. Experimental results also show that coarse-grained sand fractures more frequently than fine-grained sand. The fractures in the sand grains from reservoir sandstones, do not extend into quartz overgrowth (Fig. 8(a)), which indicates that the fractures pre-date quartz cementation. Therefore, the observed cracks in the sand grains are a result of crushing of unconsolidated sands during burial. Some deeply buried (>4.5 km) coarse-grained sandstones from Haltenbanken area contain chlorite coating and show evidence of extensive grain crushing and quartz cementation (Fig. 8(b) and (c)). The fracture network is similar to that produced experimentally at about 40 MPa (Fig. 5(f)). Extensive fracturing has taken place because grain coatings (Fig. 8(a) and (b)) have delayed quartz cementation. Fracturing in these deeply buried sandstones is likely to have occurred when the sandstones suffered an overburden of more than ~40 MPa effective stress (i.e. >4 km burial depths for hydrostatic pore pressures) during its burial. This is because mechanical compaction continued at greater depth due to lack of quartz cementation. The crushing of grains not only reduces porosity but also creates clean fracture surfaces, which provide kinetically favourable sites for quartz precipitation (Fisher & Knipe, 1998). Quartz cementation is directly proportional to surface area available for precipitation (Walderhaug, 1996) and newly created fractures provided suitable sites for quartz nucleation in the chlorite coated coarse-grained sandstones. Consequently, the coarse-grained sandstones became cemented with quartz at depths greater than 4 km. Grain fracturing, therefore, may increase the rate of quartz cementation. Extensive grain fracturing suggests that the Jurassic sandstone in well 6506/12-10 might have had close to hydrostatic pore pressures during its burial history. Well 6506/12-10 is normally pressure due to lateral drainage and there are no indications that it was previously overpressured (Olstad, 1997).

Table 2
Average number of grain contacts for different grain sizes in a sand, which is composed of 50% coarse (0.63 mm) and 50% medium (0.3 mm) grained sand

Grain size (mm)	Average grain contacts at 20 MPa	Average grain contacts at 40 MPa
0.9–1.5	5–8	7–14
0.3–0.6	3–4	3–5
< 0.1	0–2	1–3

The effect of grain crushing on compaction should be expected to be high in sandstones from sedimentary basins with a low geothermal gradient and fast rate of burial (e.g. the Gulf of Mexico, Azerbaijan and Trinidad basins) (Fisher et al., 1999). In such sandstones, strengthening of the grain framework by quartz cement does not occur until very deep burial. High overburden stresses are therefore reached prior to any quartz cementation and therefore, grain crushing could be more significant.

Deeply buried reservoirs, if overpressured, where anomalously high porosity is present due to grain coatings, may compact mechanically as fluid pressure is reduced and effective stress increased during production. A reservoir-wide collapse due to enhanced compaction during draw-down

can act to maintain the pressure drive and reduce the need for secondary recovery (e.g. Fisher et al., 1999). Further research is necessary on the importance of grain fracturing on reservoir sandstones.

4.3. Limitations of experimental compaction

The experimental compaction tests were performed at extremely high rates of loading, as high as 10^9 times the compaction rate in the Jurassic reservoir sandstones of the North Sea. Several authors (De Wall, 1996; Takei, Kusakabe, & Hayashi, 2001; Yet, Leung, & Lee, 1996) have experimentally demonstrated the time-dependent behaviour of granular material at high stresses. De Wall (1996) showed that decreasing the rate of loading enhances compaction. Yet et al. (1996) found that one possible reason for creep phenomenon might be particle breakage. However, rate of compaction decreases exponentially with time at higher stresses (Takei et al., 2001). Creep can slightly add to the amount of fracturing, but slower rate of loading can decrease fracturing. The combination of both creep and slower rate of loading can increase the overall porosity reduction in natural reservoir sandstones. The type of loading (stress system) has also been shown to be a factor in explaining the degree of grain crushing. Isotropic compression ($\sigma'_1 = \sigma'_3$; where σ'_1 and σ'_3 are major and minor principal effective stresses) suppresses grain crushing when compared with one-dimensional compression (Hardin, 1985). Another factor that influences compaction is mineral dissolution and precipitation. In the case of natural compaction in sedimentary basins, grain contact areas can be enlarged by the dissolution and precipitation of minerals reducing the grain fracturing. The experimental results presented here are valid for pure mechanical compaction. Even small amounts of mineral dissolution and precipitation (chemical compaction) may strongly influence the overall compaction.

5. Conclusions

Uni-axial compression tests on loose sands up to an effective stress level of 50 MPa show that porosity loss is a function of increasing stress, but varies greatly with grain size and grain composition.

- Coarse-grained sand shows a much higher porosity loss than medium- and fine-grained sands.
- Among the coarse-grained sands, lithic sand loses more porosity than the mono-quartz rich sand.

Thin section analyses and grain size measurements provide direct evidence of grain fracturing and crushing in sands during uni-axial compaction.

- Minor grain fracturing, probably at the grain contacts, is initiated at low stresses (2–6 MPa) and increases continuously with vertical effective stress. It becomes increasingly apparent after 10 and 20 MPa vertical effective stresses in lithic and quartzitic sands, respectively.
- At any given stress level, the degree of grain crushing is more intense in coarse-grained than in fine-grained sands. Medium-grained sand shows more fracturing than the fine-grained sand even if the porosity loss is the same.
- The degree of crushing is higher in lithic sand compared to mono-quartz rich sand.
- The higher porosity losses in the coarse- and lithic sands compared with fine- and mono-quartz rich sands (up to 25 MPa) are associated with the higher degree of grain crushing in the coarse-grained and lithic sands.
- Thin section studies from an artificially mixed sand (50/50% of 0.63 and 0.3 mm sands) shows preferential grain breakage of the grains finer than 500 μm. This is due to the lesser degree of confinement of the finer grains.

The results of experimental mechanical compaction of loose sand may provide basis to predict compaction of naturally occurring sandstones prior to quartz cementation. The overall compaction is influenced strongly by small amount of precipitation of quartz cement.

Acknowledgements

We thank Torav Berre and the technical staff of the Norwegian Geotechnical Institute (NGI) for assistance during the experiments. Caroline Lowrey is thanked for her thoughts and comments. We also appreciate the helpful suggestions from reviewer Quentin Fisher and Editor (JMPG) David Roberts. We acknowledge the financial support of the Research Council of Norway (NFR).

References

Bjørlykke, K. (1999). An overview of factors controlling rate of compaction, fluid generation and flow in sedimentary basins. In B. Jamtveit & P. Meakin, *Growth, dissolution and pattern formation in geosystems* (pp. 381–404). Dordrecht, The Netherlands: Kluwer Academic Publishers.

Boggs Jr., S. (1992). *Petrology of sedimentary rocks*, New York: Macmillan, p. 707.

Brzesowsky, R. (1995). *Micromechanics of sand grain failure and sand compaction*. PhD Thesis, University of Utrecht, The Netherlands.

Coop, M. R. (1990). The mechanics of uncemented carbonate sands. *Geotechnique*, *40*, 607–626.

Coop, M. R., & Lee, I. K. (1993). *The behaviour of granular soils at elevated stresses*, *Predictive soil mechanics*. London: Thomas Telford, pp. 186–196.

De Wall, J. A. (1996). *On the rate type compaction behaviour of sandstone reservoir rocks*, p. 165.

Dickenson, W. W., & Milliken, K. L. (1995). The diagenetic role of brittle deformation in compaction and pressure solution, Etjo Sandstones, Namibia. *Journal of Geology*, *103*, 339–347.

Fisher, Q. J., & Knipe, R. J. (1998). Fault sealing processes in siliciclastic sediments. In G. Jones, Q. J. Fisher & R. J. Knipe. *Faulting, fault sealing and fluid flow in hydrocarbon reservoirs. Special Publication of the Geological Society of London*, *147*, 117–134.

Fisher, Q. J., Casey, M., Clennell, M. B., & Knipe, R. J. (1999). Mechanical compaction of deeply buried sandstones of the North Sea. *Marine and Petroleum Geology*, *16*, 605–618.

Hagerty, M. M., Hite, D. R., Ullrich, C. R., & Hagerty, D. J. (1993). One-dimensional high pressure compression of granular material. *Journal of Geotechnical Engineering*, *119*, 1–18.

Hardin, B. O. (1985). Crushing of soil particles. *Journal of Geotechnical Engineering*, *111*, 1177–1192.

Illife, J. E., & Dawson, M. R. (1996). Basin modelling history and predictions. In K. Glennie & H. Hurst. *NW Europe's hydrocarbon industry. Geological Society London (Special Publication)*, 83–105.

Johnsen, K. L. (1985). *Contact mechanics*, London: Cambridge University Press, p. 451.

Lambe, T. W., & Whitman, R. V. (1979). *Soil mechanics*, New York: Wiley, p. 553.

Lander, R. H., & Walderhaug, O. (1999). Predicting porosity through simulating sandstones compaction and quartz cementation. *American Association of Petroleum Geologists Bulletin*, *83*, 433–449.

Laubach, S. E. (1997). A method to detect natural fracture strike in sandstones. *American Association of Petroleum Geologists Bulletin*, *81*, 604–623.

Lee, K. L., & Farhoomand, I. (1967). Compressibility and crushing of granular soil in anisotropic triaxial compression. *Canadian Geotechnical Journal*, *4*, 68–99.

Nakata, Y., Hyodo, M., Hyde, A. F. L., Kato, Y., & Murata, H. (2001). Microscopic particle crushing of sand subjected to high pressure one-dimensional compression. *Soils and Foundation*, *41*, 69–82.

Olstad, R. (1997). Porewater flow and petroleum migration in the Smørbukk field area, offshore mid-Norway. In P. M. Pedersen & A. G. Koestler. *Hydrocarbon seals: importance for exploration and production. Norwegian Petroleum Society Special Publication*, *7*, 201–217.

Pastana, J. M., & Whittle, A. J. (1995). Compression model for cohesionless soils. *Geotechnique*, *45*, 611–631.

Pittman, E. D., & Larese, R. E. (1991). Compaction of lithic sands: Experimental results and applications. *American Association of Petroleum Geologists Bulletin*, *75*, 1279–1299.

Rieke, H. H., & Chilingarian, G. V. (1974). *Compaction of argillaceous sediments*, *Developments in sedimentology*, *vol. 16*. Amsterdam: Elsevier, pp. 424.

Roberts, J. E. (1964). *Sand compression as a factor in oil field subsidence*. Unpublished PhD Thesis (pp. 306). USA: Massachusetts Institute of Technology.

Sibley, D. F., & Blatt, H. (1976). Intragranular pressure solution and cementation of the Tuscarora orthoquartizite. *Journal of Sedimentary Petrology*, *46*, 881–896.

Takei, M., Kusakabe, O., & Hayashi, T. (2001). Time-dependent behavior of crushable materials in one-dimensional compression tests. *Soil and Foundations*, *41* (1), 97–121.

Walderhaug, O. (1996). Kinetic modelling of quartz cementation and porosity loss in deeply buried sandstone reservoirs. *Bulletin of the American Association of Petroleum Geologists*, *80*, 731–745.

Yet, N. S., Leung, C. F., & Lee, F. H. (1996). Post-installation behavior of pile. *12th Southeast Asian Geotechnical Conference, Kuala Lumpur*, *vol. 1* (pp. 429–434).

Yu, Z. H., & Lerche, I. (1996). Modelling abnormal pressure developed in sandstone shale basins. *Marine and Petroleum Geology*, *13*, 179–193.

Zhang, J., Wong, T. F., & Davies, D. M. (1990a). Micromechanics of pressure-induced grain crushing in porous rocks. *Journal of Geophysical Research*, *95*, 341–352.

Zhang, J., Wong, T. F., Yanagidani, T., & Davis, D. M. (1990b). Pressure-induced microcracking and grain crushing in berea and boise sandstones: Acoustic emission and quantitative microscopy measurements. *Mechanics of Materials*, *9*, 1–15.

Zoback, M. D., & Byerlee, J. D. (1976). Effect of high pressure deformation of permeability of Ottawa sand. *American Association of Petroleum Geologists Bulletin*, *60*, 1531–1542.